TÜBİTAK

Turkish Journal of Biology

http://journals.tubitak.gov.tr/biology/

Research Article

Turk J Biol
(2018) 42: 54-62
© TÜBİTAK
doi:10.3906/biy-1710-2

Analyzing formation of silver nanoparticles from the filamentous fungus *Fusarium oxysporum* and their antimicrobial activity

Abd-Almohaimen AHMED[1], Haider HAMZAH[2,*], Mohammed MAAROOF[1]
[1]Department of Biology, College of Education for Pure Sciences, Tikrit University, Tikrit, Iraq
[2]Department of Biology, College of Science, University of Sulaimani, Sulaimani, Kurdistan Region, Iraq

Received: 03.10.2017 • **Accepted/Published Online:** 19.12.2017 • **Final Version:** 15.02.2018

Abstract: In recent years much attention has been paid to the biosynthesis of silver nanoparticles (AgNPs) and their important medical applications. The current study employs *Fusarium oxysporum* for the formation of silver nanoparticles and examines the antimicrobial activity of the particles against some multidrug-resistant (MDR) microbes. Silver nitrate was transformed into silver oxide, forming well-dispersed nanoparticles, by the action of *F. oxysporum* metabolically. The size of the nanoparticles ranged from 21.3 to 37.3 nm, and UV-spectroscopy showed a peak at 408–411 nm. Moreover, SEM, TEM, and AFM results revealed spherical and oval shapes and showed no sign of aggregation. Furthermore, the FT-IR histogram detected amide I and amide II, which are responsible for the stability of AgNPs in the aqueous solution. The AgNPs halted the growth of MDR bacteria, including some members of Enterobacteriaceae and *Staphylococcus* species at a concentration of 50% (v/v). The AgNPs also have the ability to inhibit pathogenic yeasts *Candida albicans* and *Candida krusei*. The AgNPs displayed antigrowth activity against MDR microbes, suggesting that they might be potential alternatives to antibiotics. However, additional studies may be necessary to substantiate the fact that the benefits of using nanoparticles outweigh the potential risks.

Key words: *Fusarium* species, nanotechnology, silver nanoparticles, medical applications

1. Introduction

Nanotechnology is relatively a new science of study in which a set of sciences, including the STEM (science, technology, engineering, and mathematics) disciplines, are involved to synthesize nanomaterials of about 1–100 nm. At the nanoscale level, materials have distinct chemical, physical, optical, magnetic, and electrical properties due to their large surface area to volume ratio (Chaturvedi et al., 2012). One of the most important aspects of nanotechnology is the synthesis of nanoparticles (NPs), which form the essence of nanomaterials (Ishida et al., 2014). NPs exhibit new properties based on specific characteristics such as size, distribution, and morphology. Today NPs are used in many fields, including manufacturing and materials, environmental sciences, energy and electronics, and medicine. Multidrug-resistant (MDR) microbes are a growing problem in the treatment of infectious diseases due to the widespread use of broad-spectrum antibiotics, which has resulted in the production of antibiotic resistance for many human bacterial pathogens (Franci et al., 2015). Advances in nanotechnology have opened new horizons in nanomedicine, allowing the synthesis of NPs, which are now considered a viable alternative to antibiotics and seem to have high potential in solving the problem of the emergence of microbial multidrug resistance (Rai et al., 2012).

During the last decade, increased interest has been paid to biological systems for the synthesis of NPs compared with other methods, i.e. physical and chemical methods. The latter approaches are expensive and have many limitations; therefore, scientists are developing clean, economical, and ecofriendly biological approaches as an alternative for NP synthesis (Rai et al., 2009; Seshadri et al., 2011; Wei et al., 2012). Microorganisms (mainly bacteria, yeasts, and molds) have efficiently proven their ability to absorb and accumulate inorganic metallic ions from the surrounding environment. More importantly, the ability of a biological entity to use its inherent biochemical processes to transform inorganic metallic ions into metal NPs has led to a relatively new and largely unexplored field of research. Among microbes, filamentous fungi are widely used as biocatalysts in NP preparation (Mukherjee et al., 2002; Sawle et al., 2008). In addition to heavy metal tolerance, fungi have the ability to produce

* Correspondence: haider.hamzah@univsul.edu.iq

higher amounts of proteins, leading to higher rates of NP synthesis (Mohanpuria et al., 2008). Several papers have been published describing the synthesis of silver NPs using mycosynthesis (Ahmad et al., 2003; Mishra et al., 2011; Soni et al., 2012; Gopinath et al., 2015); however, there is a continuing effort throughout the world to exploit fungal species in the nanotechnology field. A few reports have been published about nonpathogenic filamentous fungus *Fusarium* species and their capabilities in reducing aqueous silver ions extracellularly to generate silver NPs (Durán et al., 2005; Ahmad et al., 2010). However, these previous studies did not cover the broad spectrum of silver NPs synthesized by the action of *F. oxysporum* against pathogenic bacteria and pathogenic yeasts.

In this study, the tested hypothesis is that a local isolate of filamentous fungus *F. oxysporum* tolerates heavy metals and actively synthesizes silver NPs extracellularly. Therefore, the main objectives of the present study were using *F. oxysporum* as a biocatalyst for the synthesis of NPs and investigation of their antimicrobial activity against some MDR isolates.

2. Materials and methods

2.1. Synthesis of AgNPs

A local isolate of *F. oxysporum* (F2A) was used for the synthesis of silver nanoparticles (AgNPs). Colonies of *F. oxysporum* were grown on potato dextrose agar (PDA) plates for 6 days at 28 °C and were used to inoculate 250 mL of MYPG medium (consisting of 3 g malt extract, 3 g yeast extract, 2 g peptone, and 10 g glucose per liter) in Erlenmeyer flasks. The flasks were incubated at 28 °C for 7 days with shaking at 150 rpm. Mycelial pads were harvested aseptically and washed 3 times with distilled water. The biomass of fungi was weighed and then used for the synthesis of nanoparticles applying an approach similar to that of Ahmad et al. (2003) and Durán et al. (2005) with some modifications. Briefly, three Erlenmeyer flasks were prepared; the first one contained 10 g of wet biomass and 100 mL of sterile distilled water and this flask was used as a negative control. The second flask included 10 g of mycelium pad and 100 mL of 1 mM silver nitrate (the metal solution was sterilized with a 0.22-µm Millipore filter). The third flask was also used as a negative control since it contained 100 mL of metal solution only. All flasks were incubated at 28 °C in the dark for 190 h with shaking at 150 rpm. Filtration and then centrifugation (at 5000 rpm for 20 min) were carried out, and then the supernatants were characterized.

2.2. Characterization of AgNPs

The synthesized NPs were characterized based on specific surface plasmon resonance peak, shape, size, and interaction between protein and NPs**.** To confirm the synthesis of AgNPs, 2 mL of sample was measured spectrophotometrically at a wavelength ranging from 300–600 using a Genesys 6 spectrophotometer (Thermo Electron, USA). Considering that the primary goal of this study was to produce a powerful antimicrobial nanomaterial, the agar well diffusion method was conducted to learn the antimicrobial properties of the NPs. Briefly, pathogenic bacterial isolates (*Escherichia coli*, *Staphylococcus epidermidis*, and *Staphylococcus aureus*) were grown in nutrient broth for 24 h at 37 °C. The number of cells per milliliter was adjusted to be 10^8 in a plate count procedure; 100 µL of inoculum (1×10^8 cells/mL) was swabbed onto Mueller Hinton agar plates. Wells were made using gel puncture and then 0.1 mL of different dilutions of AgNPs (10%, 25%, 50%, 75%, and 100%) was loaded into certain wells. The plates were incubated at 37 °C overnight and then the zone of inhibition was measured (mm). This experiment was performed three times and then averages and standard deviations were calculated using Microsoft Excel. In accordance with the collected results of the agar well diffusion method, the NPs were subjected to microscopic identification via SEM (CamScan 3200LV, UK) and TEM (Philips CM10, the Netherlands) (procedure modified from Gurunathan et al., 2009). To confirm the formation of AgNPs, atomic force microscopy (AFM; Phywe measure Nano, UK) was used. To identify the presence of possible biomolecules, Fourier transmission infrared spectroscopy (FT-IR; WQF-520 Biotech, UK) was applied.

2.3. Antimicrobial activity of AgNPs

All pathogenic microbes obtained from Sulaimani Teaching Hospitals in Kurdistan Region, Iraq, were MDR. The activity of AgNPs was tested against pathogenic microbes using growth inhibition by using microtiter plate. Growth inhibition assays were performed on *Escherichia coli*, *Enterobacter cloacae*, *Klebsiella pneumoniae*, *Proteus mirabilis*, *Pseudomonas aeruginosa*, *Staphylococcus aureus*, and *Staphylococcus epidermidis*. Fresh overnight cultures of pathogenic bacterial isolates were adjusted to be 10^8 cells/mL as mentioned previously. A bacterial culture of 120 µL was placed in 96-well microtiter plates and then 80 µL of an appropriate dilution of AgNPs (25%, 50%, 75%, and 100%) was added. Nutrient broth (200 µL) was used as a negative control and 120 µL of bacterial culture mixed with 80 µL of fungal extract was also applied as a negative control. The microtiter plates were incubated at 37 °C for 18 h (modified procedure of Salem et al., 2015). The optical density (OD) at 600 nm was measured using a microplate spectrophotometer (Biotech µQuant, USA). From each well, 5 µL was taken and spotted onto nutrient agar plates, and then all plates were incubated at 37 °C for 18 h. Growth percentage was calculated based on the average and standard deviation of triplicate results. For pathogenic fungi (*Candida albicans* and *Candida krusei*),

the same method as mentioned above was used, except that the medium was replaced with potato dextrose broth and PDA. The number of cells per milliliter was adjusted to be 10^6 using a hemocytometer.

3. Results

3.1. Synthesis and characterization of AgNPs

F2A was able to convert $AgNO_3$ into AgNPs after 190 h of incubation as noticed visually by color change from white to light brown, whereas the control vessels developed no change in their original color (Figure 1; inset). The wavelength scan of UV-Vis spectra revealed a broad peak between 408 and 411 nm, indicating the surface plasmon resonance nature of the AgNPs that is present in the brown supernatant (Figure 1).

Interestingly, the colored solution of AgNPs displayed a powerful inhibition against the clinical isolates (Figure 2). Bacterial growth was inhibited even at the lowest concentration. From the average values of inhibition zones (Figure 2, insets), the highest antimicrobial activity was observed against *S. epidermidis*, which was 14 mm in diameter, whereas the cultures of *S. aureus* and *E. coli* also showed clear zones of inhibition, which were about 13 and 12.25 mm in diameter, respectively. Moderate antibacterial activity was noticed at a lower concentration of AgNPs (25%), while it was weak in 10% AgNPs against the tested bacteria.

SEM was used to determine the presence and size of AgNPs. After drying, the thin layer of AgNPs was analyzed. The scanning electron micrograph showed the presence of high-density AgNPs with mainly spherical shape (Figure 3A, white arrows). The data obtained from TEM micrographs show that the synthesized AgNPs have a spherical shape and the size ranged from 21.3 to 37.3 nm, uniformly distributed without significant agglomeration (Figure 3B, black arrows). A two-dimensional horizontal cross-section of the AgNPs by AFM indicated that the surface topography of the synthesized silver nanoparticles was almost spherical in shape (Figure 3C). Histogram analysis revealed that the mean particle size was approximately 21.5 nm.

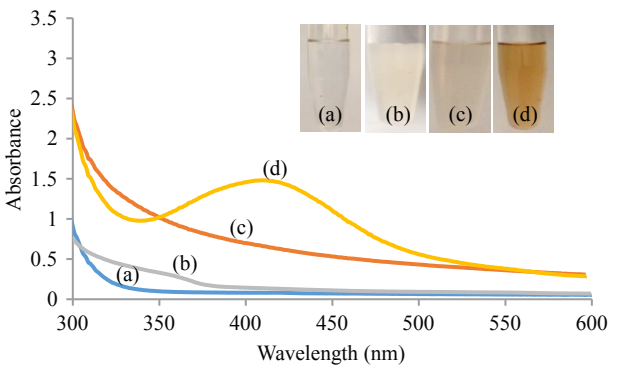

Figure 1. UV-Visible absorption spectra of AgNPs: a) $AgNO_3$ solution (1 mM) control; b) biomass of F2A test sample before incubation, c) supernatant of (F2A) control, d) biomass of (F2A) test sample. Inset: Color change of filtrate from white (b) to light brown (treated) after synthesis of AgNPs (d).

The absorption peaks of AgNPs (Figure 4) are located at 538, 679, 768, 847, 1070, 1340, 1432, 1516, 1630, 2943, and 3411 cm^{-1} in the region of 500–400 cm^{-1}. The band at 1630 cm^{-1} is assigned to the stretching vibration of -C=O (carbonyl), identified as the amide I band, whereas the bands at 3411 cm^{-1} and 1516 cm^{-1} represent stretching and bending vibrations of -NH, respectively.

3.2. Antimicrobial activity of AgNPs

The effectiveness of AgNPs on MDR clinical isolates was determined by comparing growth rates under control and test conditions (Figures 5–7). AgNPs showed antimicrobial properties against all tested microbes; however, their exact effect on microbes was not clearly understood and was not investigated in this study. As seen in Figure 5, at a concentration of 25% (v/v) AgNPs, *Enterobacter cloacae*, *E. coli*, *Pseudomonas aeruginosa*, and *Klebsiella pneumoniae* were inhibited significantly, whereas 25% AgNP concentration showed no significant effect on *Proteus mirabilis*. In addition, similar behavior was exhibited at 25% and 50% concentrations against both *Pseudomonas aeruginosa* and *Klebsiella pneumoniae*.

All gram-negative bacteria used here were inhibited significantly; the highest antimicrobial activity was observed against *E. coli* and *Proteus mirabilis*, whose growths were restrained at the AgNP concentration of 50%. On the other hand, at a relatively high concentration (75%) of AgNPs, the growth of the other isolates was suppressed. In Figure 6, two gram-positive bacteria are shown. The concentration of AgNPs also halted the growth of these bacteria. It seems that *S. epidermidis* tolerates up to about 50% of AgNPs in comparison with *S. aureus*.

In Figure 7, the fungicidal effect is observed at a concentration of 50% (v/v) against *Candida albicans* while *Candida krusei* showed a high degree of resistance.

4. Discussion

Many questions remain unanswered about the resistance mechanisms of fungal strains towards many inhibitors such as heavy metals. Although fungi possess many properties that influence metal toxicity, the mechanisms involved in metal tolerance are highly dependent on the metabolic and nutritional status of the organism (Salem et al., 2015). In this study, silver nitrate has halted the growth of 7 species of *Fusarium* except the F2A isolate (data not shown); F2A survived the effects of 1 mM silver. F2A might develop a new survival strategy as an adaptive response to unfavorable environmental conditions.

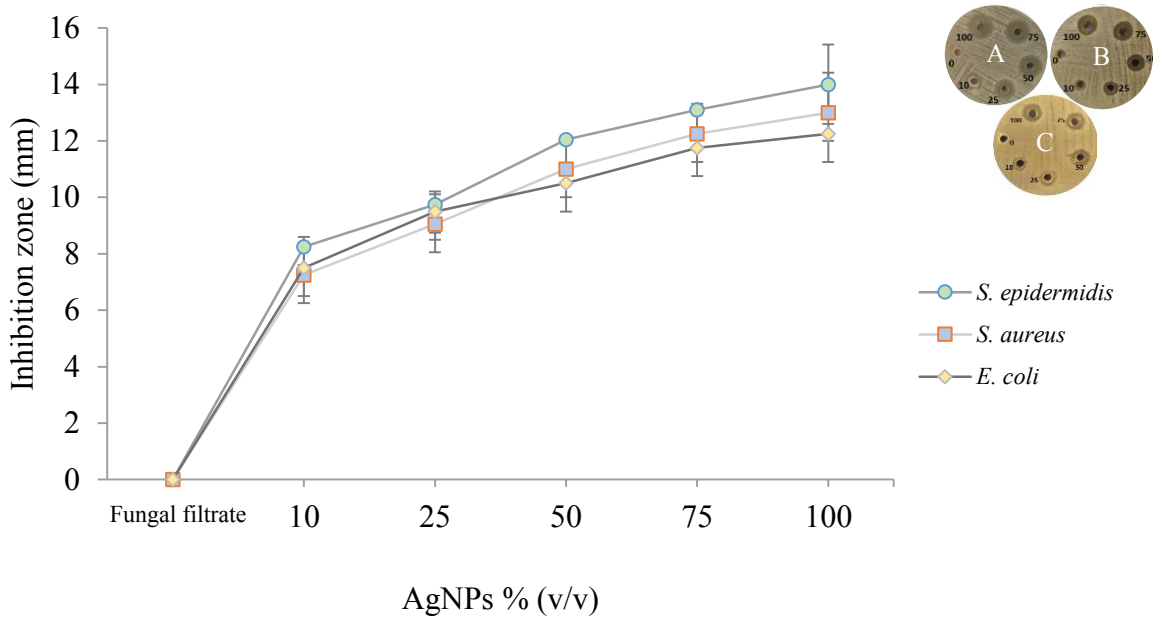

Figure 2. Inhibition zone assay of clinical isolates by synthesized AgNPs. Inset: A) *S. epidermidis*; B) *S. aureus*; C) *E. coli*.

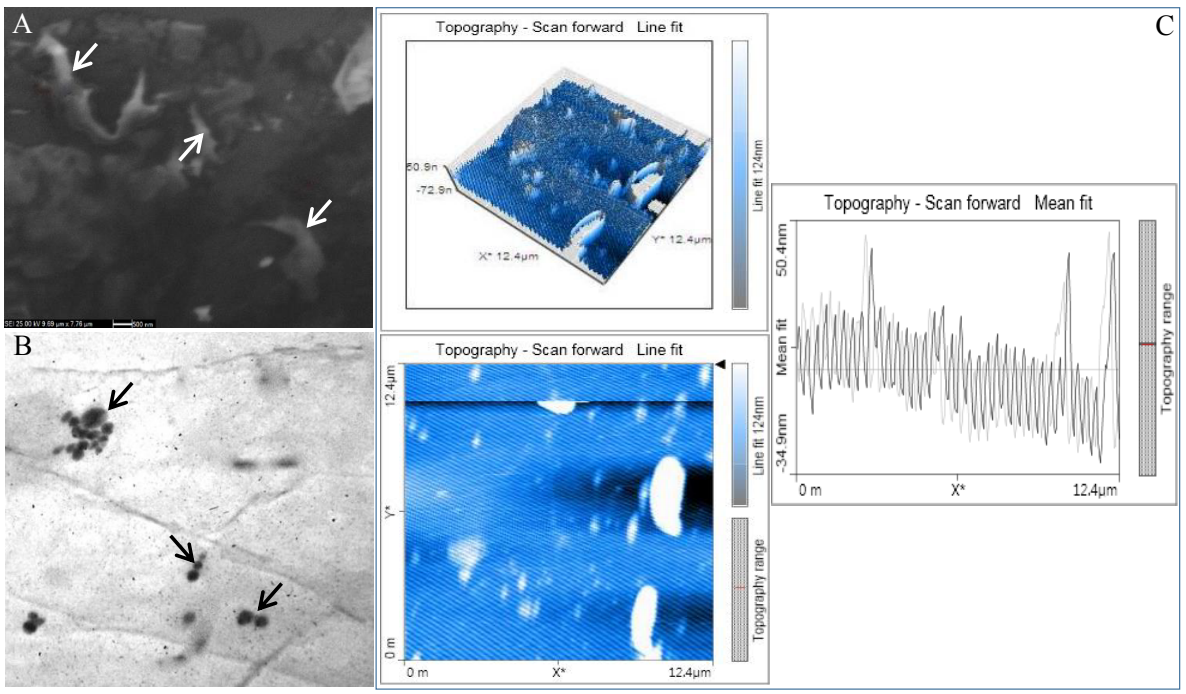

Figure 3. Micrograph of AgNPs synthesized by F2A: A) SEM image, B) TEM image, C) AFM image. Left upper picture depicts the 3D image of the AgNPs whereas left lower picture represents the 2D image of the AgNP horizontal cross-section. Right image indicates the histogram analysis, showing average particle size of 21.5 nm.

Consequently, F2A was selected as a biocatalyst for the synthesis of AgNPs. F2A was able to reduce silver ions to silver NPs since it is well known that AgNPs in aqueous solutions show a yellowish brown color (Ahmad et al., 2003). This bioreduction occurred through catalysis by the reducing agent secreted from the F2A biomass into the solution. *Fusarium* species have been used previously for NP production (Ahmad et al., 2003; Durán et al., 2005;

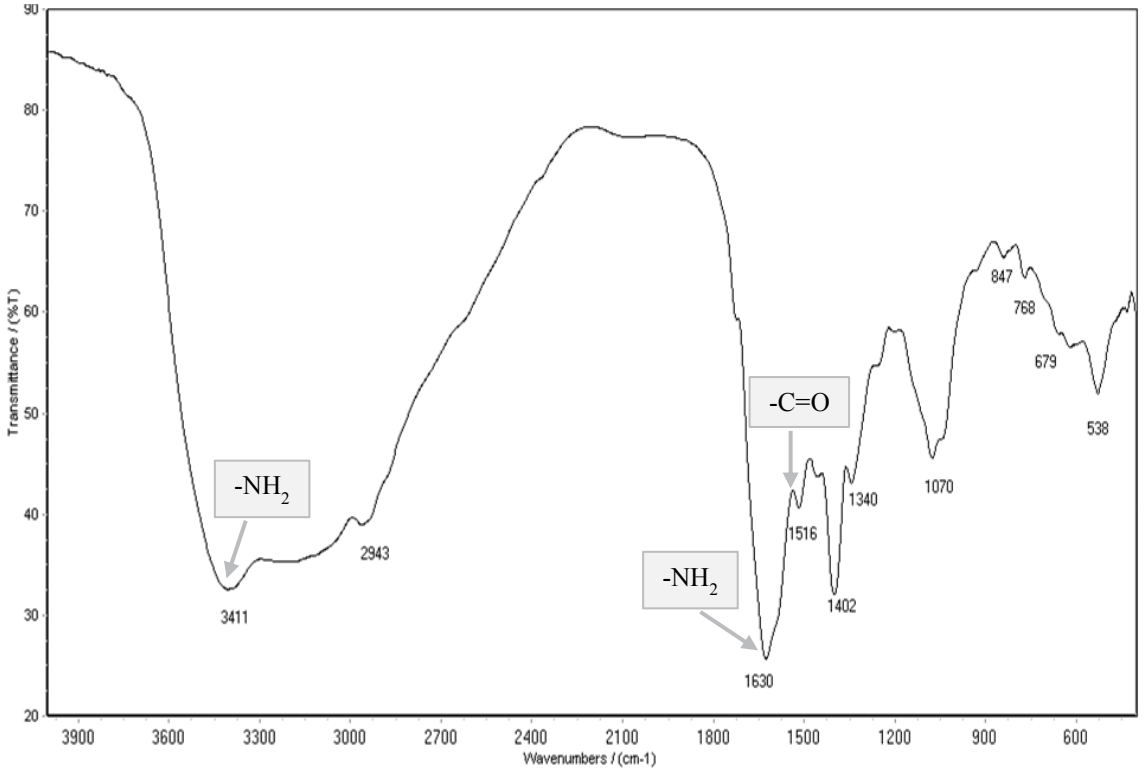

Figure 4. FT-IR spectrum of silver nanoparticles synthesized by F2A. Gray boxes depict both amide I (-C=O) and amide II (-NH) bands.

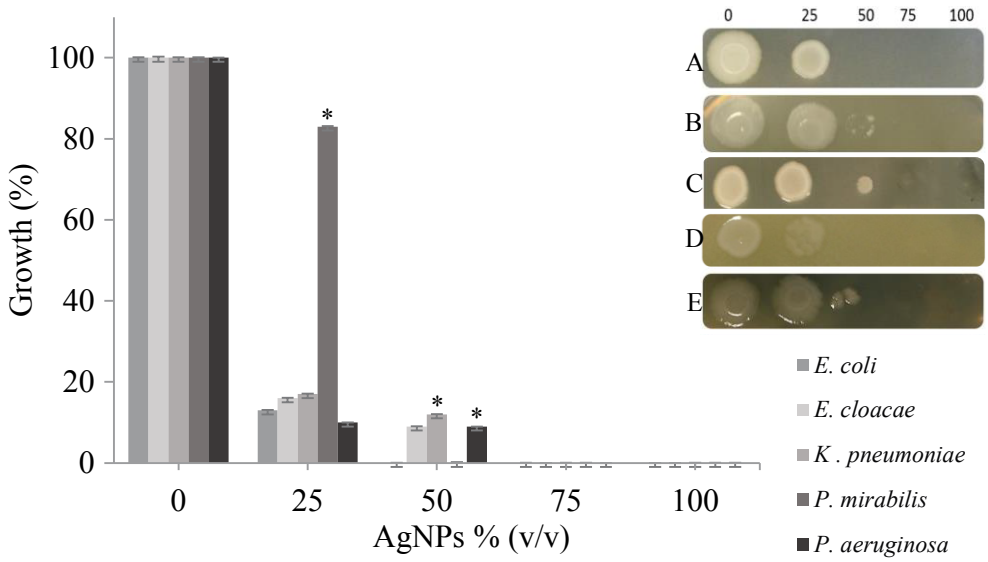

Figure 5. Growth inhibition assay using microtiter plate technique. Inset: 5 µL was taken from each well and spotted onto nutrient agar plates. A) *E. coli*; B) *Enterobacter cloacae*; C) *Klebsiella pneumoniae*; D) *Proteus mirabilis*; E) *Pseudomonas aeruginosa*.

Gadd, 2007); however, previous studies did not cover the broad spectrum of silver NPs synthesized by the action of *F. oxysporum* against pathogenic bacteria and pathogenic fungi. The slow silver reduction (~190 h) could be the result of unfavorable growth conditions, due to the presence of relatively high concentrations of silver nitrate.

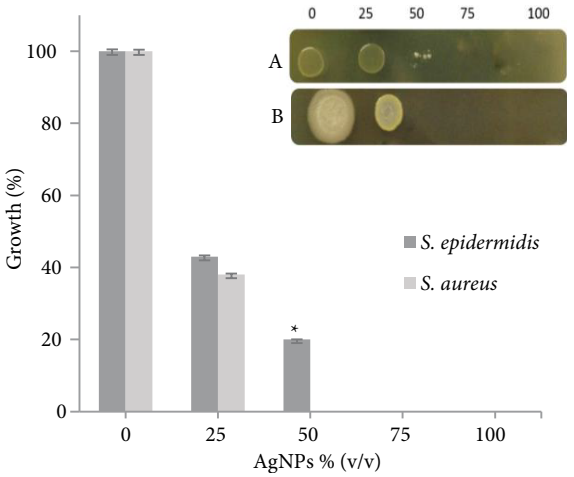

Figure 6. Growth inhibition assay using microtiter plate. Inset: 5 µL was taken from each well and spotted onto nutrient agar plates. A) *S. epidermidis*; B). *S. aureus*.

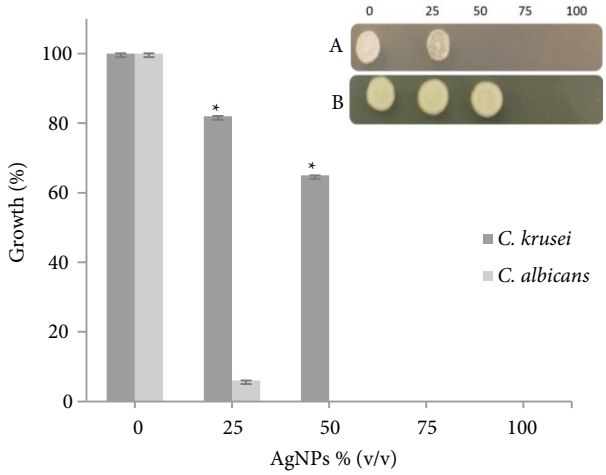

Figure 7. Growth inhibition assay using microtiter plate. Inset: 5 µL was taken from each well and spotted onto PDA plates. A) *Candida albicans*; B) *Candida krusei*.

The formation of silver NPs might occur by the action of reductase enzyme(s) excreted during fungal growth phases (Durán et al., 2005). However, the restricted growth rate of the fungus in such batch cultures may perhaps lead to the delayed excretion of the enzyme(s), which leads to the slow reduction of silver nitrate. Notably, this long period of time gives stable AgNPs, as mentioned below. Thereafter, the colored solution was tested and analyzed spectrophotometrically using UV-Vis in the scan range of 300–600 nm (Figure 1). Interestingly, AgNPs absorbed light at different wavelengths and were excited due to charge density at the interface between conductor and insulator to give a respective peak on UV-Vis spectrophotometry (Gurunathan et al., 2015), which is in agreement with several other studies (Rodríguez-León et al., 2013; Kumar et al., 2016). These results suggest that the biopolymer protein plays a key role in providing stability to AgNPs. The biopolymer forms a ligand-shell surrounding AgNPs at the core, forming a silver polymer core-shell structure. The polymeric shell decreases the surface potential that is responsible for accumulation of the silver nanoparticles to larger aggregates (Busi et al., 2014).

Frequently, microbes are considered dead when they cannot be cultured. However, variation in the size of inhibition zones depends upon a number of factors such as the type of pathogens, synthesis method, and concentrations of AgNPs. It was observed in this study that increasing the concentration (v/v) of AgNPs in wells led to consistently increasing zones of inhibition (Figure 2). At 40 mg/mL, AgNPs showed a good inhibitory zone against various pathogenic bacteria (Gopinath et al., 2015; Sanyasi et al., 2016). Gopinath et al. (2015) showed that the shapes of AgNPs synthesized by *F. oxysporum* were spherical to oval in shape with little aggregation. The SEM micrographs of silver NPs show aggregated particles due to the capping agent(s), mainly metabolites of the action of microbes (Figure 3A). Therefore, the particle sizes measured by SEM can be larger than the sizes measured by TEM or XRD (Durán et al., 2005). TEM images have provided evidence of extracellular synthesis of AgNPs (Kowalczyk et al., 2011). TEM is widely used to analyze the structure and size of NPs and in this study it was used to determine the size and shape of silver NPs (Figure 3B). Basavaraja et al. (2008) synthesized AgNPs ranging from 8 to 60 nm with polydispersity and mostly spherical in shape. Ahmad et al. (2003) obtained AgNPs with a size of 5–50 nm with a spherical shape. Together, SEM and TEM analysis provide further insight into the morphology and particle size distribution profile of the AgNPs synthesized by *F. oxysporum*. Besides SEM and TEM techniques, AFM was used to obtain information about the effect of solution chemistry on the AgNPs' dissolution kinetics. In this case, aggregation cannot occur because the particles are immobilized. AFM is an obvious choice for characterizing dissolutive changes in the size and shape of AgNPs since it can resolve sample topography with subnanometer precision. The three-dimensional images showed the average roughness and inhomogeneity of the cluster formation of AgNPs (Figure 3C). On the other hand, Majeed et al. (2016) showed that AgNPs were spherical and 30–50 nm in size. FT-IR measurement was performed to identify the possible biomolecules responsible for the capping and efficient stabilization of the metal nanoparticles and to understand the protein/metal NP interaction. The FT-IR spectroscopic analysis clearly reveals that proteins are responsible for the reduction and stabilization of AgNPs

(Figure 4). Many studies have proved that bands at 1516 cm^{-1} in addition to C=O (carbonyl) stretching and –N–H– stretching vibrations correspond to the amide linkages of proteins (Hamedi et al., 2014; Luna et al., 2016). Hamedi et al. (2014) showed that the appearance of peaks in the amide I and amide II regions describes proteins and/or enzymes that have been found to be responsible for the reduction of metal ions when using microorganisms as biocatalysts. It seems that the F2A metabolites play dual functions in the formation and stabilization of AgNPs.

In the 1940s, western industries began to focus on the production of fungal-specific secondary metabolites by the cultivation of the fungi on relatively raw materials using submerged and solid state cultures. Since then, tremendous medically significant metabolites (such as antibiotics) are being produced, purified, and sold for medicinal purposes. Antibacterial activities of AgNPs in this report have been investigated against MDR gram-positive and gram-negative bacteria (Figures 5 and 6). This resistance might be attributed to the presence of a self-produced extracellular matrix in both isolates and its roles in the defense mechanisms (Jagnow et al., 2003; Periasamy et al., 2015). Moreover, cells may be inactive or damaged and therefore unable to reproduce temporarily. With time and appropriate conditions, the cells may recover and begin to reproduce. The presence of multiple mechanisms to avoid inhibitors in some clinical strains allow them to survive and resist the most commonly used drugs. This tolerance could be due to specific antibiotic resistance genes and the formation of biofilms (Otto, 2009). Although the inhibition of bacterial growth indicates that AgNPs possess a bactericidal property, the mechanisms that contribute to cell death remain vague. One hypothesis is that AgNPs are involved in the disruption of the membrane with a generation of reactive oxygen species and ultimately lead to the death of pathogens (Prabhu and Poulose, 2012). Another possibility is that AgNPs have the ability to adhere to the bacterial cell wall and produce cracks and pits, through which the internal cell contents are released (Feng et al., 2000). The efficacy of AgNPs against pathogenic yeasts was evaluated by identifying growth percentage in a 96-well microtiter plate. More importantly, the AgNPs produced by *F. oxysporum* exhibited potent antifungal activity against two species of *Candida* (Figure 7). Although *Candida krusei* is an uncommon clinical isolate, it does tolerate a broad array of antifungals (Pfaller et al., 2008). Therefore, finding a robust agent is necessary for many opportunistic pathogens like *Candida krusei*. A previous study showed that AgNPs biosynthesized by the fungus *Arthroderma fulvum* showed considerable antifungal activity against *Candida* species (Xue et al., 2016). Lara et al. (2015) found that AgNPs caused severe morphological changes in fungal cells manifested by disruption of the cell membrane structure.

In conclusion, the AgNPs synthesized by *F. oxysporum* were characterized as spherical to oval in shape with average size ranging between 21.5 and 37.3 nm. The AgNPs remained stable with a slight change in color. However, the peak of surface plasmon resonance remained unchanged with the same region after storage for 4 months under 4 °C cooling conditions (data not shown). Obviously, pathogenic bacteria continue to develop resistance to a long list of antibiotics, leading to untreatable infections. AgNP-producing F2A shows promise as an effective biocatalyst and its Ag nanoparticles have powerful lethality against MDR microbes. AgNPs showed inhibitory effects against all MDR bacteria used in this study. AgNPs also displayed antifungal activity against pathogenic yeasts. For future work, the toxicity of AgNPs needs to be studied to establish that the benefits of using nanoparticles outweigh the potential risks.

Acknowledgments

The authors would like to thank Adiba Sharif at Sulaimani Technical Institute for her valuable help in doing some fungal experiments. The authors also thank the staff of the Central Service Laboratory at the University of Baghdad for assisting with AFM and FT-IR analysis. We acknowledge the staff of the Kurdistan Institution for Strategic Studies and Scientific Research for their help during SEM analysis. We are grateful to the staff of the Chemistry Department at Nahrain University for helping with TEM examinations.

References

Ahmad A, Mukherjee P, Senapati S, Mandal D, Khan MI, Kumar R, Sastry M (2003). Extracellular biosynthesis of silver nanoparticles using the fungus *Fusarium oxysporum*. Colloid Surface B 28: 313-318.

Ahmad M, Al-Salhi MS, Siddiqui MKJ (2010). Silver nanoparticles applications and human health. Clin Chim Acta 411: 1841-1848.

Basavaraja SS, Balaji SD, Lagashetty AK, Rajasab AH, Venkataraman A (2008). Extracellular biosynthesis of silver nanoparticles using the fungus *Fusarium semitectum*. Mater Res Bull 43: 1164-1170.

Busi S, Rajkumari J, Karuganti S, Ranjan B (2014). Green rapid biogenic synthesis of bioactive silver nanoparticles (AgNPs) using *Pseudomonas aeruginosa*. IET Nanobiotechnol 8: 267-274.

Chaturvedi S, Dave PN, Shah NK (2012). Applications of nano-catalyst in new era. J Saudi Chem Soc 16: 307-325.

Durán N, Marcato PD, Alves OL, De Souza GIH, Esposito E (2005). Mechanistic aspects of biosynthesis of silver nanoparticles by several *Fusarium oxysporum* strains. J Nanobiotech 3: 8.

Feng QL, Wu J, Chen GQ (2000). A mechanistic study of the antibacterial effect of silver ions on *Escherichia coli* and *Staphylococcus aureus*. J Biomed Mater Res 52: 662-668.

Franci G, Falanga A, Galdiero S, Palomba L, Rai M, Morelli G, Galdiero M (2015). Silver nanoparticles as potential antibacterial agents. Molecules 20: 8856-8874.

Gadd GM (2007). Geomycology: biogeochemical transformations of rocks, minerals, metals and radionuclides by fungi, bioweathering and bioremediation. Mycol Res 111: 3-49.

Gopinath PM, Narchonai G, Dhanasekaran D, Ranjani A, Thajuddin N (2015). Mycosynthesis, characterization and antibacterial properties of AgNPs against multidrug resistant (MDR) bacterial pathogens of female infertility cases. Asian J Pharm Sci 10: 138-145.

Gurunathan S, Jeong JK, Han JW, Zhang XF, Park JH, Kim JH (2015). Multidimensional effects of biologically synthesized silver nanoparticles in *Helicobacter pylori*, *Helicobacter felis*, and human lung (L132) and lung carcinoma A549 cells. Nanoscale Res Lett 10: 35.

Gurunathan S, Kalishwaralal K, Vaidyanathan R, Venkataraman D, Pandian SRK, Muniyandi J, Hariharan N, Eom SH (2009). Biosynthesis, purification and characterization of silver nanoparticles using *Escherichia coli*. Colloid Surface B 74: 328-335.

Hamedi S, Shojaosadati SA, Shokrollahzadeh S, Hashemi-Najafabadi S (2014). Extracellular biosynthesis of silver nanoparticles using a novel and non-pathogenic fungus, *Neurospora intermedia*: controlled synthesis and antibacterial activity. World J Microbiol Biotechnol 30: 693-704.

Ishida K, Cipriano TF, Rocha GM, Weissmuller I, Gomes F, Miranda K, Rozental S (2014). Silver nanoparticle production by the fungus *Fusarium oxysporum*: nanoparticles characterization and analysis of antifungal activity against pathogenic yeasts. Mem Inst Oswaldo Cruz 109: 220-228.

Jagnow J, Clegg S (2003). *Klebsiella pneumoniae* MrkD-mediated biofilm formation on extracellular matrix- and collagen-coated surfaces. Microbiology 149: 2397-2405.

Kowalczyk B, Lagzi I, Grzybowski BA (2011). Nanoseparations: strategies for size and/or shape-selective purification of nanoparticles. Curr Opin Colloid In 16: 135-148.

Kumar CMK, Yugandhar P, Savithramma N (2016). Biological synthesis of silver nanoparticles from *Adansonia digitata* L. fruit pulp extract, characterization, and its antimicrobial properties. J Intercult Ethnopharmacol 5: 79.

Lara HH, Romero-Urbina DG, Pierce C, Lopez-Ribot JL, Arellano-Jiménez MJ, Jose-Yacaman M (2015). Effect of silver nanoparticles on *Candida albicans* biofilms: an ultrastructural study. J Nanobiotechnol 13: 91.

Luna C, Barriga-Castro ED, Gómez-Treviño A, Núñez NO, Mendoza-Reséndez R (2016). Microstructural, spectroscopic, and antibacterial properties of silver-based hybrid nanostructures biosynthesized using extracts of coriander leaves and seeds. Int J Nanomedicine 11: 4787.

Majeed S, bin Abdullah MS, Nanda A, Ansari MT (2016). In vitro study of the antibacterial and anticancer activities of silver nanoparticles synthesized from *Penicillium brevicompactum* (MTCC-1999). Journal of Taibah University for Science 10: 614-620.

Mishra A, Tripathy SK, Yun S (2011). Biosynthesis of gold and silver nanoparticles from *Candida guilliermondii* and their antimicrobial effect against pathogenic bacteria. J Nanosci Nanotechnol 11: 243-248.

Mohanpuria P, Rana NK, Yadav SK (2008). Biosynthesis of nanoparticles: technological concepts and future applications. J Nanopart Res 10: 507-517.

Mukherjee P, Senapati S, Mandal D, Ahmad A, Khan MI, Kumar R, Sastry M (2002). Extracellular synthesis of gold nanoparticles by the fungus *Fusarium oxysporum*. Chem Bio Chem 3: 461-463.

Otto M (2009). *Staphylococcus epidermidis*-the "accidental" pathogen. Nat Rev Microbiol 7: 555-567.

Periasamy S, Nair HAS, Lee KWK, Ong J, Goh JQJ, Kjelleberg S, Rice SA (2015). *Pseudomonas aeruginosa* PAO1 exopolysaccharides are important for mixed species biofilm community development and stress tolerance. Front Microbiol 6: 851.

Pfaller MA, Diekema DJ, Gibbs DL, Newell VA, Nagy E, Dobiasova S (2008). *Candida krusei*, a multidrug-resistant opportunistic fungal pathogen: Geographic and temporal trends from the ARTEMIS DISK antifungal surveillance program, 2001 to 2005. J Clin Microbiol 46: 515-521.

Prabhu S, Poulose EK (2012). Silver nanoparticles: mechanism of antimicrobial action, synthesis, medical applications, and toxicity effects. Int Nano Lett 2: 32.

Rai M, Yadav A, Gade A (2009). Silver nanoparticles as a new generation of antimicrobials. Biotechnol Adv 27: 76-83.

Rai MK, Deshmukh SD, Ingle AP, Gade AK (2012). Silver nanoparticles: The powerful nanoweapon against multidrug-resistant bacteria. J Appl Microbiol 112: 841-852.

Rodríguez-León E, Iñiguez-Palomares R, Navarro RE, Herrera-Urbina R, Tánori J, Iñiguez-Palomares C, Maldonado A (2013). Synthesis of silver nanoparticles using reducing agents obtained from natural sources (*Rumex hymenosepalus* extracts). Nanoscale Res Lett 8: 318.

Salem W, Leitner DR, Zingl FG, Schratter G, Prassl R, Goessler W, Reidl J, Schild S (2015). Antibacterial activity of silver and zinc nanoparticles against *Vibrio cholerae* and enterotoxic *Escherichia coli*. Int J Medical Microbiol 305: 85-95.

Sanyasi S, Majhi RK, Kumar S, Mishra M, Ghosh A, Suar M, Satyam PV, Mohapatra H, Goswami C, Goswami L (2016). Polysaccharide-capped silver nanoparticles inhibit biofilm formation and eliminate multidrug- resistant bacteria by disrupting bacterial cytoskeleton with reduced cytotoxicity towards mammalian cells. Sci Rep 6: 24929.

Sawle BD, Salimath B, Deshpande R, Bedre MD, Prabhakar KB, Venkataraman A (2008). Biosynthesis and stabilization of Au and Au-Ag alloy nanoparticles by fungus, *F. semitectum*. Sci Technol Adv Mater 9: 035012.

Seshadri S, Saranya K, Kowshik M (2011). Green synthesis of lead sulfide nanoparticles by the lead resistant marine yeast, *Rhodosporidium diobovatum*. Biotechnol Prog 27: 1464-1469.

Soni N, Prakash S (2012). Efficacy of fungus mediated silver and gold nanoparticles against *Aedes aegypti* larvae. Parasitol Res 110: 175-184.

Wei X, Luo M, Lietal W (2012). Synthesis of silver nanoparticles by solar irradiation of cell-free *Bacillus amyloliquefaciens* extracts and $AgNO_3$. Bioresour Technol 103: 273-278.

Xue B, He D, Gao S, Wang D, Yokoyama K, Wang L (2016). Biosynthesis of silver nanoparticles by the fungus *Arthroderma fulvum* and its antifungal activity against genera of *Candida*, *Aspergillus* and *Fusarium*. Int J Nanomedicine 11: 1899.